Rev. Téc. Ing. Univ. Zulia. Vol. 30, Nº 1, 23 - 32, 2007

Flame speed oscillations in combustion of two-phase mixtures

F. Atzler[1], F.X. Demoulin[2], M. Lawes[2], Y. Lee[3] and N. Marquez[4]

[1]*Basic Combustion, Siemens VDO Automotive AG. 93055 Regensburg, Germany.*
[2]*School of Mechanical Engineering, University of Leeds. Leeds, LS2 9JT, UK.*
[3]*Engine R&D Center, Environment & Energy Division, Korea Institute of Machinery and Materials. 171 Jang-dong Youseong-ku Daejeon Korea 305-343.*
[4]*Escuela de Ingeniería Mecánica, Universidad del Zulia, Apartado 526. Maracaibo 4011-A, Venezuela. numarquez@luz.edu.ve*

Abstract

The phenomenon of flame oscillation, the cyclic variation of flame speed during flame development, has been studied in the past in clouds of dust or droplets and even in gaseous mixtures. Although it has been addressed in the past using several approaches there is no yet a unique accepted explanation. In the present work, drop inertia effects were investigated, by comparing the experimental data with modelled predictions of oscillations in flame speed caused by the aerodynamic interaction of the gas motion ahead of the flame front with the drops. The combustion studies of nearly mono-sized droplet clouds in the present work revealed the differences between the speed of droplets and the gas velocity near the flame front. These resulted in variations in local equivalence ratio, which in turn manifested in flame speed oscillations. For simplification a combustion vessel has been used to study the combustion of droplet clouds from a fundamental point of view, under strictly controlled (accurately established) conditions of pressure, temperature and equivalence ratio. The distribution of droplets within the mixture (spatially and in time), without combustion, was characterised somewhere else.

Keywords: Flame speed, oscillations, droplet cloud.

Oscilaciones en la velocidad de propagación en la combustión de mezclas de dos fases

Resumen

El fenómeno de oscilación en llamas: variación cíclica de la velocidad de propagación durante el desarrollo de la llama, ha sido estudiado en el pasado en nubes de polvo o gotas e incluso en mezclas gaseosas. A pesar de que el fenomeno ha sido estudiado desde diferentes perspectivas aún no hay una explicación única aceptada. En el presente trabajo, los efectos de la inercia de los gotas fueron investigados, comparando los datos experimentales con predicciones de modelos de oscilacion de velocidad de llama causada por la interaccion aerodinamica del movimiento del gas cercano al frente de llama con las gotas. Los estudios de combustión del presente trabajo, en nubes con tamaño de gota casi único, pusieron de manifiesto la diferencia entre la velocidad de las gotas y la velocidad cerca del frente de llama. Esta diferencia produjo variación en la relación de equivalencia local que a su vez se manifestó en oscilaciones de la velocidad de propagación. Por simplicidad se ha utilizado para las pruebas, un equipo que permite estudios fundamentales de la combustión en nubes de gotas, bajo condiciones estrictamente controladas (establecidas en forma precisa) de presión, temperatura y relación de equivalencia. La distribución de las gotas dentro de la mezcla sin combustión se caracterizó en otro estudio.

Palabras clave: Velocidad de propagación, oscilaciones, nube de gotas.

1. Introduction

An instability associated to two-phase combustion is that of flame speed oscillation. Many studies have been aimed to identify the mechanisms responsible for this phenomenon in order to suppress it, given the negative effects of pulses in a stable/continuous flow/flame, however the mechanisms are unclear yet. The interaction with acoustic waves is possible [1]. Other researchers [2] observed similar oscillations in flames expanding in a cloud of solid polymethylmethacrylate (PMMA) and attributed them to radiation effects. Another mechanism may be due to thermo-diffusive or hydrodynamic cellular instabilities, which are a function of flame stretch and Markstein length [3-5]. A fourth possible mechanism for the oscillations is the variations in equivalence ratio due to phase lags between flame and droplet velocities. This has been investigated in the present work.

The presence of fuel droplets complicates the study of combustion processes because of the time required to evaporate and mix the liquid fuel with the surrounding medium and because of the difference between the velocity of the liquid and gas phases.

Results obtained from experiments that simulate industrial applications are in many cases apparatus specific. The fan stirred bomb used in the present work has been developed [3, 4] to produce fundamental data and due to its excellent optical access facilitates the use of laser diagnostics.

The present work reports two-phase combustion data for conditions that are difficult to attain by other techniques. These include data at low temperatures down to 265 K which are relevant to aircraft engines at altitude relight conditions.

2. Burning Velocity Determination

Following mixture preparation as described in Atzler *et al.* [6], flames were initiated by central spark ignition. The procedure for obtaining the flame speed and burning velocity were similar to those used for gaseous mixtures [3, 4, 7]. The flame speed of an aerosol mixture, as a function of flame radius, time and stretch, was obtained from photographic observation (schlieren) of the spherically expanding flame. The stretched flame speed, S_n, is given by

$$S_n = dr_f \,/\, dt \tag{1}$$

and the stretch rate on a flame of surface area, $A = 4\pi r_f^2$, is

$$\alpha = \frac{1}{A}\frac{dA}{dt} = \frac{2}{r_f}\frac{dr_f}{dt} = \frac{2}{r_f}S_n. \tag{2}$$

The unstretched laminar flame speed, S_s is obtained by extrapolating a curve of S_n against stretch to zero, and the gradient of this curve yields the burned gas Markstein length, L_b, such that

$$S_n = S_s - \alpha L_b. \tag{3}$$

However, for several flames reported in this work neither S_s nor L_b could be determined, due to the strong oscillations in S_n.

3. Experimental Apparatus and Techniques

The combustion vessel and auxiliary equipment for the preparation and combustion of droplet clouds have been described in Atzler *et al.* [6] and are shown schematically in Figure 1. The combustion vessel is a cylindrical bomb of 305 mm diameter by 305 mm developed by Abdel-Gayed *et al.* [3], which was used only to study the burning of gases and dusts [8]. Windows installed in both end plates provided optical access for various laser diagnostics. The initial conditions of temperature were reached using two electrical heaters attached to the end plates. During the mixture preparation in this work, four internal fans, driven by adjustable speed motors were used. The apparatus was modified by Atzler and Lawes [9] to produce aerosols mixtures expanding the initial gaseous mixture to a second vessel (expansion vessel).

The aerosol mixture preparation has been described in Atzler *et al.* [6]. This method also known as the Wilson cloud chamber technique [10], has been used in combustion studies by

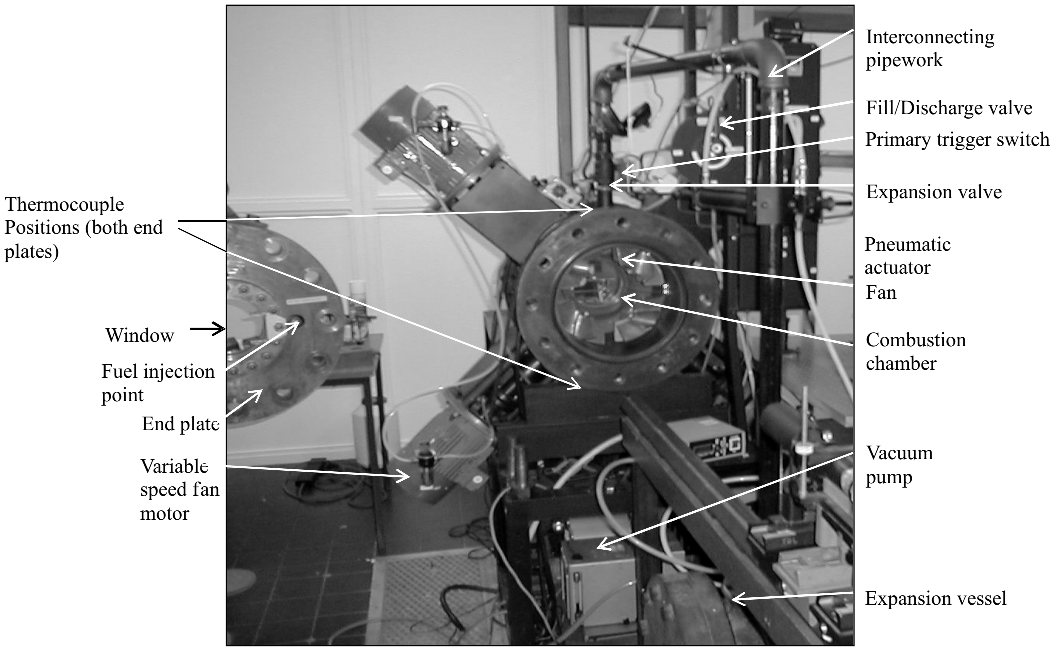

Figure 1. Experimental apparatus for droplet cloud combustion.

Hayashi *et al.* [11] and Nakabe *et al.* [12]. The procedure includes: evacuate both the combustion and expansion vessel then isolate the combustion vessel from the expansion vessel, prepare a gaseous pre-mixture in the combustion vessel, injecting liquid iso-octane and air to achieve the desired equivalence ratio and initial pressure. The fans were run to aid in complete the evaporation of the liquid fuel and also in the mixing. Afterward, the fans were stopped. Before igniting the mixture, this was allowed to vent, at a controlled rate, through an orifice into the expansion vessel. The result is a reduction in mixture pressure and temperature that took it into the wet regime (fuel droplets were formed). The initial pressure, temperature and rate of expansion determined the conditions at the ignition time (and during combustion), such as pressure, temperature, liquid and gaseous phase equivalence ratio, droplet diameter distribution and number density as discussed in Atzler *et al.* [6]. A spark of approximately 400 mJ initiated central ignition.

To cover a wide range of initial conditions for combustion studies the characteristics of this mixture were required to vary, changing the initial conditions before expansion or the ignition time. Ignition conditions were defined based on the temporal variation of droplet Sauter mean diameter, D_{32} , pressure, temperature, mass fraction of liquid fuel and equivalence ratio, all identified by Atzler *et al.* [6].

For droplet velocity determination a different technique than schlieren was required, as droplets could not be visualised with the last. Laser sheet imaging and Particle Image Velocimetry (PIV), were used for this purpose. Due to the experimental variability between single experiments it was necessary to record simultaneously schlieren and laser sheet imaging to verify relative velocities.

The experimental apparatus for laser sheet imaging and schlieren is shown in Figure 2. The laser sheet was generated using a Oxford lasers, LS-20-50, Cu-vapour laser (510 nm) and associated optics to produce a 30 mm wide by 0.2 mm thick sheet at the centre of the vessel. A Cordin, Model 321, Drum camera with Nikon zoom lens was used to record sheet images of droplets. A 510 nm interference filter, placed in front of the camera was used to discriminate between the sheet image and background illumination. Typically, 43 images at a framing rate of 2 kHz were recorded per combustion experiment. A 10 mW, He-Ne laser (632 nm) was used to provide high speed schlieren movies simultaneously with the laser sheet imaging movies. For this, dichroic

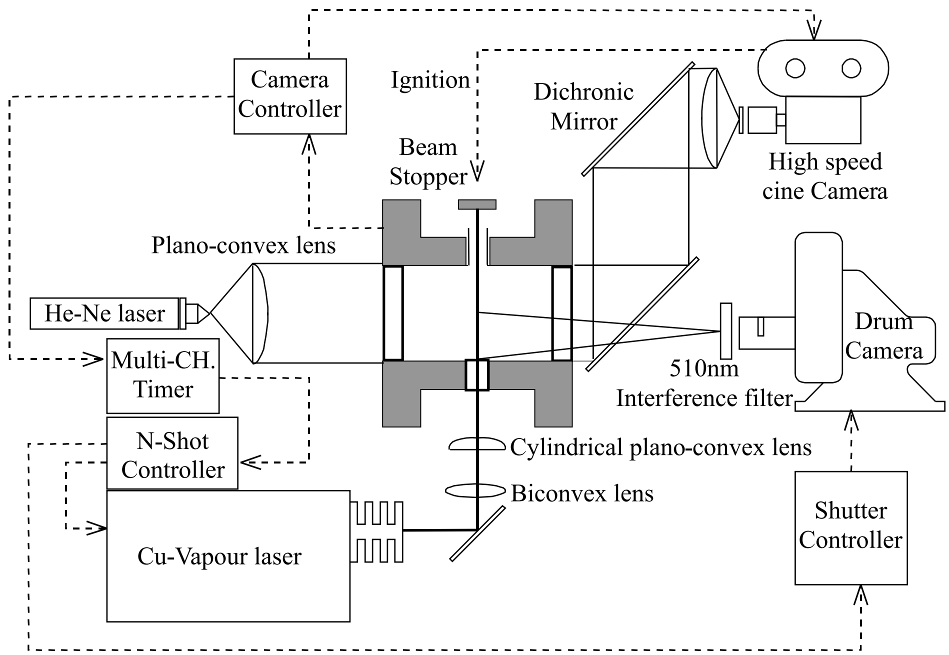

Figure 2. Experimental apparatus for simultaneous schlieren flame photography and PIV imaging.

mirrors were installed to reflect the schlieren beam onto a Hitachi high speed 16 mm camera while transmitting the laser sheet images onto the drum camera. Number density calculation requires laser attenuation measurements as described in Atzler *et al.* [6], the beam described for the schlieren technique was used and the high speed camera was replaced by a laser power meter.

4. Combustion Studies

This work presents results of oscillating flames and compare them with other non oscillating cases, looking for a possible explanation of this phenomenon. All flames were ignited at a selection of initial conditions taken from Atzler *et al.* [6] which shows that the present vessel effectively provides a wide range of two phase mixtures within which combustion studies can be undertaken and which depends on the initial gaseous conditions of pressure, temperature and equivalence ratio and on the time between the start of expansion and flame initiation. The combustion event is significantly faster (typically, 50 ms) than droplets development during condensation (about one second). Hence, droplet size and distribution can be assumed to be the same as those at ignition, and the evaporation of droplets at or near the flame front can be assumed instantaneous.

Shown in Figure 3 is the variation of flame speed with time from ignition. Data for overall equivalence ratios, $_{ov}$, of 1.0 and 0.8 are presented. For each, two gaseous phase equivalence ratios, $_{g}$, are shown such that the effect of liquid fraction/D_{32} could be investigated. For the cases in which $_{g}$ is closest to $_{ov}$, (the smallest liquid fraction/D_{32}) the flame speed increased with time in much the same way as that observed for gaseous mixtures [7]. After a period of time during which the effect of spark ignition diminished, a flame was established and this propagated and accelerated as the stretch decreased (radius increased). As illustrated by the two cases in Figure 3 in which the liquid fraction was highest (lowest $_{g}$) for the given $_{ov}$, when the proportion of liquid was increased, the flame speed oscillated between maxima and minima. Moreover, as shown in Figure 4 for the case of $_{ov}$ = 1.0 and $_{g}$ = 0.66, schlieren photographs revealed that the structure of these flames also oscillated between smooth and cellular. Although mild oscillations have been observed in gaseous flames [7], and cellular instabilities are well understood [5] such strong oscillations in flame speed and structure as those in Figures 3 and 4 have not been re-

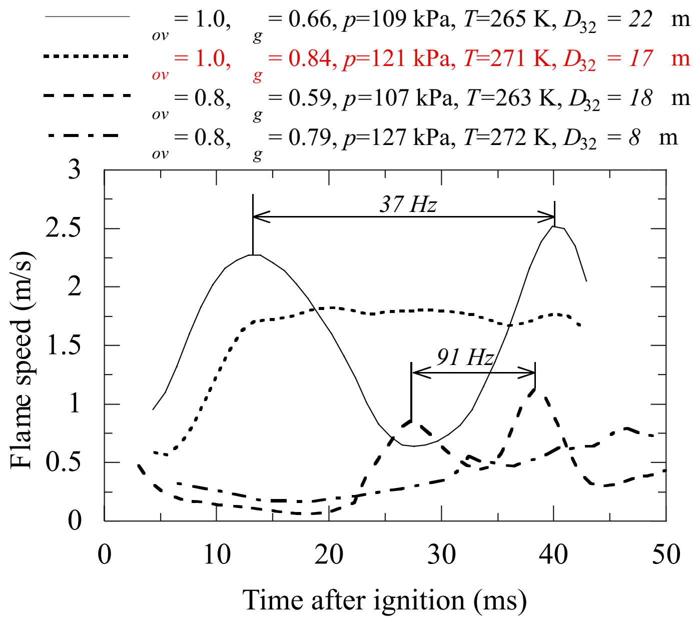

Figure 3. Variation of flame speed with time from ignition for various iso-octane – aerosol mixtures.

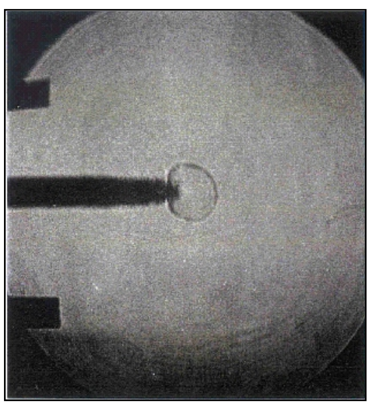

t = 5ms r_f = 9 mm (smooth)

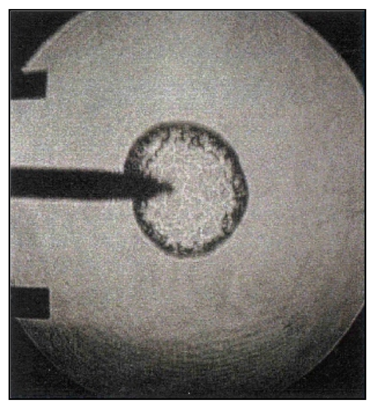

t = 11ms r_f = 22 mm (cellular)

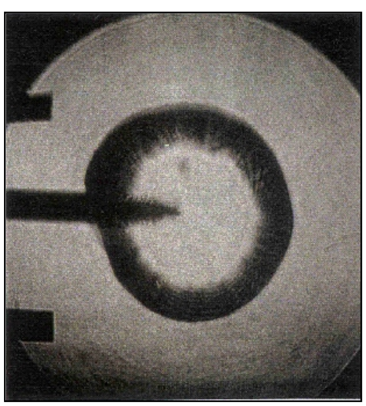

t = 21ms r_f = 35 mm (smooth)

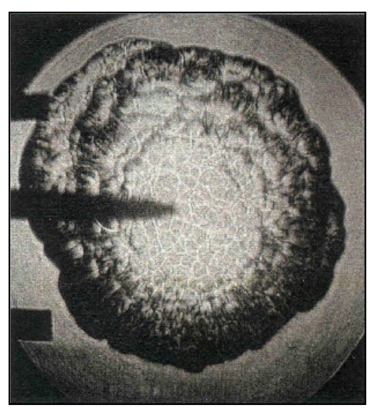

t = 38 ms r_f = 53 mm (cellular)

Figure 4. Schlieren images of flame propagation. Initial conditions are: 109 kPa, 265 K, $_{ov}$ = 1.0, $_g$ = 0.66, and D_{32} = 22 μm.

ported elsewhere. The mechanisms for such oscillations are unclear. As mentioned before, the interaction with acoustic waves is possible [1]. However, as shown in Figure 4, the frequency of the oscillations is less than 100 Hz while the frequency of an acoustic wave, assuming a characteristic length equal to that of the vessel at the given conditions, is about 900 Hz. Another explanation is that given by Hanai *et al.* [2] whom observed similar oscillations in flames expanding in a cloud of solid PMMA and attributed them to radiation effects. However, it is unlikely that radiation effects will be significant here because droplets evaporate within, or before, the flame zone [13]. The other mechanism already mentioned is due to thermo-diffusive or hydrodynamic cellular instabilities, which are a function of flame stretch and Markstein length [3-5]. However, it is not clear if the production/destruction of the cellular structure is a cause or effect of the oscillations in flame speed [13]. Another mechanism that could trigger oscillations is the variations in equivalence ratio due to phase lags between flame and droplet velocities. This is investigated below.

Effect of droplet inertia on the equivalence ratio of a spray flame

Due to the difference between the velocity of the liquid and gas phases and also the time required to evaporate and mix the liquid fuel with the surrounding there might be locally differences in the equivalence ratio of the burning mixture, obviously this is affected by the amount of liquid present. In the present work, drop inertia effects were investigated, by comparing the experimental data with modelled predictions of oscillations in flame speed caused by the aerodynamic interaction of the gas motion ahead of the flame front with the drops. This model was developed by Atzler *et al.* [14] and the main assumptions used are: the two phase mixture was considered initially quiescent and homogeneous in which the fuel droplets were vaporised only in the preheat zone of the flame, that vaporisation was complete, and that gaseous mixing was instantaneous. Due to the expanding flame, the velocity of the gas that surrounds the droplets is not constant and a varying drag force exists. Droplet inertia results in a lag between the gas and droplet velocities.

The flame speed depends on the equivalence ratio in the reaction zone and this depends on the number density of droplets that enter it. During a time interval, *dt*, the flame propagates through a volume of gas, $V_g = A\,u_n\,dt$, where u_n is the stretched laminar burning velocity. During this time, the number of droplets entrained into the flame, *N*, is given by

$$N = n_L A(S_n - u_d)dt\,, \tag{4}$$

where n_L is the droplet number density at the leading edge of the flame, and u_d is the droplet velocity at the same point and S_n was defined for Equation (1). Thus the number density of droplets that enter the flame, n_f, is

$$n_f = n_L\left(\frac{S_n - u_d}{u_n}\right). \tag{5}$$

The overall equivalence ratio of the two-phase mixture at any point before ignition is given by

$$\phi_{ov} = \phi_g + \phi_l, \tag{6}$$

where $_l$ is the liquid equivalence ratio. However, the total equivalence ratio within the reaction zone would be changing from that value depending on the number of droplets caught into the flame or the ratio of number densities at the flame and away from it, as in the expression

$$f = \phi_g + \frac{n_L}{n_{dr}}(\phi_{ov} - \phi_g)\left(\frac{S_n - u_d}{u_n}\right), \tag{7}$$

where n_{dr} is the number density remote from the flame. Three limiting cases are revealed from Equation (7):

1. Clearly, cannot be less than $_g$. If $u_d > S_n$, then the droplets move away from the flame, n_L reduces to zero and the initial gaseous phase equivalence ratio results.
2. If u_d = the gas velocity, $u_g = S_n - u_n$, then the term in the second set of brackets becomes unity, $n_L = n$ and, hence, $= _{ov}$. This corresponds to the case in which the droplets have negligible inertia.
3. If $u_d = 0$, the equivalence ratio attains a maximum and we obtain:

$$\phi_{\max} = \phi_g + \frac{\rho_u}{\rho_b}(\phi_{ov} - \phi_g).$$

This corresponds to the case in which the droplets have infinite inertia. Since $_u/\ _b > 1$, $_{max} >\ _{ov}$.

To investigate the proposal that droplet inertia can lead to flame speed oscillations, the equivalence ratio from Equation (7) was calculated using estimated values of flame speed and burning velocity. For a spray flame the laminar burning velocity was assumed to be that of a gaseous flame with the same values of and rate of stretch, based on the results of Lawes *et al.* [15].

The unstretched flame speed is related to the laminar (unstretched) burning velocity, u_l, by

$$u_l = S_s \rho_b / \rho_u , \qquad (8)$$

where $_b$ and $_u$ are the burnt and unburnt gas densities.

Because of the condensation method used to create the spray, the unburnt gas temperature was low and, by definition, it was not possible to have an equilibrium gaseous mixture at the same pressure, temperature and equivalence ratio as those of the spray. Therefore, the unstretched laminar burning velocity was estimated using the relationship:

$$u_l = u_{l,0}(T_u / 358)^{2.1}, \qquad (9)$$

in which $u_{l,0}$ is the unstretched laminar burning velocity at 1 bar and 358 K. This, approximate relationship was proposed by Lawes *et al.* [15] for iso-octane mixtures at pressures close to 1 bar and for temperatures down to 260 K. The stretched flame speed, S_n, was obtained from Equation (3). From measurements obtained by Bradley *et al.* [7], an approximate value for L_b, for conditions in the present work, is given by

$$L_b = 13.604\phi^2 - 36.535\phi + 24.324. \qquad (10)$$

The gas velocity just ahead of the flame front is equal to

$$u_g = S_n - u_n , \qquad (11)$$

and u_n is approximated by

$$S_n = (\rho_u / \rho_b) u_n . \qquad (12)$$

Equation (7) is an intrinsic equation in which the burning velocity is an input that depends on the output equivalence ratio. The flame speed was estimated by assuming that there was no variation in pressure, temperature and equivalence ratio that would affect burning velocity during the short period of flame propagation. Shown in Figure 5 is a graphical representation of the solution of Equation (7) for $_{ov}$ = 1 and $_g$ = 0.66.

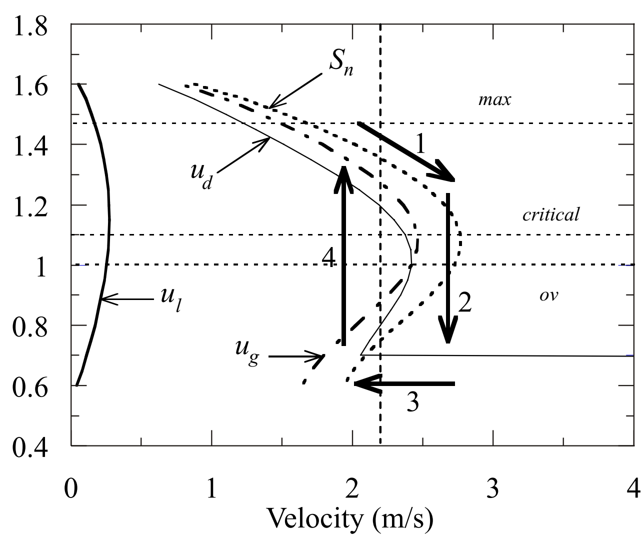

Figure 5. Graphical representation of Equation 7. Variations of S_n, u_g, u_l and u_d with when $_{ov}$ = 1 and $_g$ = 0.66.

It shows the variations of , S_n, u_g and u_l as a function of droplet velocity. At low droplet velocities, there is a unique solution. For droplet velocities between about 2 and 2.5 ms^{-1}, there are three solutions. The vertical dashed line at 2.2 ms^{-1} is an example of these cases. For the highest value of obtained at 2.2 ms^{-1}, if increases, the burning velocity reduces. Hence, fewer droplets are entrained and reduces again to complete a cycle of deceleration and acceleration. Similarly, the lowest value of obtained at 2.2 ms^{-1}, yields a unique value of burning velocity for any value of droplet velocity in that range, the mentioned solutions are considered stables. However, the middle value corresponds to a range of in which the burning velocity increases with . In this range, if increases, the burning velocity increases, more droplets are entrained into the flame and increases further. Similarly, if decreases, the burning velocity decreases, fewer droplets are entrained and decreases further. Hence, this solution is unstable.

Figure 5 shows a possible mechanism to explain the pulsating expanding spherical flame. Initially, following ignition, the droplet velocities near the flame front are equal to zero. Therefore, the equivalence ratio in the reaction zone is $\phi_{\max}$. The flame causes a gas velocity ahead of the flame front and the droplets accelerate due to the drag force. Hence, fewer droplets are entrained by the flame and the equivalence ratio decreases as in regime 1. As the stoichiometric equivalence ratio is approached, the droplets continue to accelerate towards that of the gas velocity, while the burning velocity and gas velocities reduce as their peak values, at the critical equivalence ratio, $_{critical}$, are passed (regime 2). At $_{ov}$ =1.0, the droplet and gas velocities become equal. After this, inertia results in droplet velocities that are higher than the gas velocity as the latter continues to reduce. Therefore, the equivalence ratio within the reaction zone tends towards = $_g$ (regime 3), but would attain this value when $u_d = S_n$. Eventually, the droplets approach equilibrium with the surrounding gas and more droplets are entrained as begins to increase through $_{ov}$ and $_{critical}$ (regime 4) as the droplets once again lag behind the gas velocity. The cycle then is repeated.

A necessary condition for this mechanism is that $_{ov}$, at which the droplet velocities are equal to the gas velocity, must be less than $_{critical}$. If $_{ov}$, were greater than $_{critical}$, then as the droplet and gas velocities became equal at $_{ov}$, the burning velocity and gas velocity still would be accelerating as $_{critical}$ was approached. Hence, it would be unlikely that the droplet velocity would exceed the gas velocity and steady state would be attained at $_{ov}$. This critical value occurs at approximately = 1.1 for iso-octane [7]. Hence, it might be expected that flame oscillations, by the proposed mechanism, occur when $_{ov}$ <1.1.

Experimental support for the proposed mechanism is presented in Figure 6 in which flame speed and droplet speed are compared as functions of flame radius. The solid curve in Figure 6 is for the flame at $_{ov}$ = 1.0 and $_g$ = 0.66. The droplet velocity at the leading edge of the flame is shown by the circles and was obtained by particle image velocimetry analysis of temporally resolved laser sheet images. Shown by the dashed-dotted line is the variation of gas phase velocity and this was estimated using Equation (11). Between radii of 16 and 33 mm, the droplet velocity is lower than the gas velocity and accelerates towards it. During this period, the flame speed is high, reflecting the increased equivalence ratio.

Between approximately 33 and 40 mm, the droplet velocity is higher than the gas velocity which results in reductions in and, hence, S_n. At 40 mm, the largest radius at which droplet velocity was measured, the droplet velocity again falls below that of the gas velocity and the cycle repeats. Shown by the dotted lines in Figure 6 are the variations of the flame speed of gaseous phase iso-octane and air at equivalence ratios equal to those of $_{critical}$ = 1.1 and $_g$. Both the minimum and maximum values of flame speed for the aerosol mixture are in reasonable agreement with those for the gaseous phase mixture at $_g$, and $_{critical}$ as expected from the analysis above.

5. Conclusions

Fundamental studies of the combustion of two phase mixtures requires well defined experi-

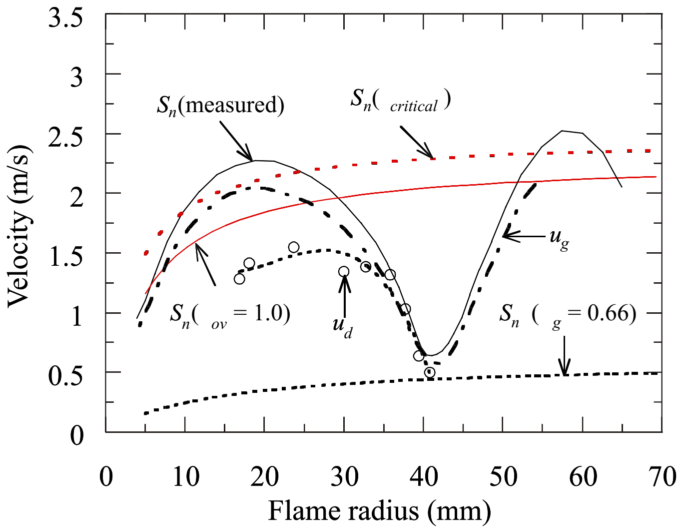

Figure 6. Variation of flame speed and droplet velocity (at the flame front) with flame radius for the flame in Figure 5.

ments in which all relevant parameters can be adequately controlled and measured. To this end, an experimental apparatus has been developed and calibrated such that spatially homogeneous aerosol mixtures can be investigated with a variety of traditional and laser diagnostics.

Measurements of the propagation of laminar aerosol flames revealed oscillations in their flame speed. A simple model is proposed to explain the oscillations in terms of droplet inertia. Due to inertia, the real equivalence ratio within the reaction zone can be larger or smaller than the overall equivalence ratio. This influences the flame speed and can lead to oscillations. These oscillations result in burning rates that, locally, can be higher or smaller than that at the overall equivalence ratio. The minimum burning velocity is equivalent to that of a gaseous flame with an equivalence ratio equal to $_g$. The maximum burning rate can correspond to that of a gaseous flame that is richer than the overall equivalence ratio of the spray. The modelled predictions were verified experimentally by comparing gaseous velocities with those of the droplets.

List of Symbols

A	flame surface area (m^2)
D	droplet diameter (m)
L_b	burned gas Markstein length (mm)
N	number of droplets
n	number density of droplets (m^{-3})
r_f	flame radius (mm)
p	pressure (kPa)
S	flame speed (m/s)
t	time (s)
T	temperature (K)
u	burning velocity, velocity (m/s)
V	volume (m^3)
	stretch (s^{-1})
ρ	density (kg/m^3)
ϕ	equivalence ratio
	Subscripts:
a	air
b	burned
d	droplets
dr	remote from the flame
f	flame, fuel
g	gas
l	liquid, laminar
L	leading edge of the flame
max	maximum
n	stretched
o	original, reference condition
ov	overall
s	unstretched

u unburned

32 Sauter-mean diameter

Abbreviations:

PIV particle image velocimetry

PMMA polymethylmethacrylate

References

1. Clavin P.; Sung J. (1991) Theory of acoustic instabilities of planar flames propagating in sprays or particle-laden gases, Combustion Science & Technology, 78, 265-288.
2. Hanai H.; Maruta K.; Kobayashi H.; Niioka T. (1998) Pulsating Flame Propagation of PMMA Particle Cloud in Microgravity, 27th Symp. (Int.) on Combustion, The Combustion Institute, pp. 2675-2681.
3. Abdel-Gayed R.G.; Al-Kishali K.J.; Bradley D. (1984) Turbulent burning velocities and flame straining in explosions, Proceedings of the Royal Society, London, A 391: 393-414.
4. Gillespie L.; Lawes M.; Sheppard C.G.W.; Woolley R. (2001) 'Aspects of Laminar and Turbulent Burning Velocity Relevant to SI Engines', SAE 2000 Transactions, Volume 109, Journal of Engines, Section 3, pp: 13-33 (2001).
5. Bradley D.; Sheppard C.G.W.; Woolley R.; Greenhalgh D.A.; Lockett R.D. (2000) The Development and Structure of Flame Instability and Cellularity at Low Markstein Numbers in Explosions, Combustion and Flame, 122:195-209.
6. Atzler F.; Lawes M.; Lee Y.; Marquez N. (2005) Characterization of two-phase combustible mixtures produced in a fan stirred bomb. Rev. Téc. Fac. Ing. LUZ. To be published.
7. Bradley D.; Hicks R.A.; Lawes M.; Sheppard C.G.W.; Woolley R. (1998) The Measurement of Laminar Burning Velocities and Markstein Numbers for Iso-octane-Air and Iso-octane-N-heptane-Air Mixtures at Elevated Temperatures and Pressures in an Explosion Bomb, Combustion and Flame, 115: 126-144.
8. Swithenbank J.R. (1987) The Fundamentals of Dust Explosions, PhD thesis, Department of Mechanical Engineering, University of Leeds.
9. Atzler F.; Lawes M. (1998), Burning velocities in droplet suspensions. Proc. 14th Int. Conference On Liquid Atomisation and Spray Systems, pp. 578-583.
10. Wilson C.T.R. (1911) On a method of Making Visible the Paths of Ionising Particles Through a Gas, Proceedings of the Royal Society, London, A85, pp. 285-288.
11. Hayashi S.; Kumagai S.; Sakai T. (1976) Propagation Velocity and Structure of Flames in Droplet-Vapour-Air Mixtures, Combustion Science & Technology, 15: 169-177.
12. Nakabe K.; Mizutani Y.; Akamatsu F.; Fuchihata M.; Elemam S.H. (1991) Spark Ignited Spherical Flames Propagating in a Suspended Droplet Cloud, NIST Special Publications, 5th Int. Conference on Liquid Atomisation and Spray Systems ICLASS-91, Gaithersburg.
13. Márquez-Montero N.E. (2003) Fundamental studies of aerosol flames, PhD thesis, Department of Mechanical Engineering, University of Leeds.
14. Atzler F.; Demoulin F.X.; Lawes M.; Lee Y. (2001) Oscillations in the flame speed of globally homogeneous two phase mixtures, 18th International Colloquium on the Dynamics of Explosions and Reactive Systems. 29 July-4 Aug.
15. Lawes M.; Marquez-Montero N.E.; Lee Y. (2002) Enhanced burning rates due to droplet induced flame instabilities, Proceedings of the 18th International conference on liquid atomization and spray systems, ILASS-Europe2002, Zaragoza, 9-11th September, 2002.

Recibido el 31 de Octubre de 2005
En forma revisada el 23 de Febrero de 2007